Acta Pharmacologica Sinica (2010) 31: 531–539
 1671-4083/10 $32.00
www.nature.com/aps

Original Article

Expression of a dominant-negative Rho-kinase promotes neurite outgrowth in a microenvironment mimicking injured central nervous system

Ping YANG*, Hui-zhong WEN, Jin-hai ZHANG

Department of Neurobiology, the Third Military Medical University, Chongqing 400038, China

Aim: To investigate whether lentiviral vector (LV)-mediated expression of a dominant negative mutant Rho-kinase (DNROCK) could inhibit activation of the Rho/ROCK signaling pathway and promote neurite outgrowth in a hostile microenvironment mimicking the injured central nervous system (CNS) *in vitro*.

Methods: Lentiviral stock was produced using the three-plasmid system by transfecting HEK293 cells. Myelin prepared from rat brain was purified by two rounds of discontinuous density gradient centrifugation and osmotic disintegration. Differentiated PC12 cells and dissociated adult rat dorsal root ganglion (DRG) neurons were transduced with either LV/DNROCK or LV/green fluorescent protein (GFP) and seeded on solubilized myelin proteins. The effect of DNROCK on growth cone morphology was tested by rhodamine-conjugated phalloidin staining. Expression of DNROCK was determined by immunoblotting. The length of the longest neurite, the percentage of neurite-bearing neurons, or the total process outgrowth for all transduced neurons were measured by using the Scion image analysis program.

Results: Transduction of DNROCK inhibited serum-induced stress fiber formation in NIH 3T3 cells and induced enlargement of cell bodies and decreased the phosphorylation levels of MYPT1 in HeLa cells. LV/DNROCK blocked myelin-induced increase in ROCK translocation from cytosol to membrane in LV/GFP-treated PC12 cells. DNROCK promotes neurite outgrowth of differentiated PC12 cells and DRG neurons on myelin protein. LV/DNROCK-transduced PC12 cells had longer neurites than LV/GFP-transduced cells (39.18±2.19 μm *vs* 29.32±1.7 μm, $P<0.01$) on myelin-coated coverslips. Furthermore, a significantly higher percentage of LV/DNROCK-transduced cells had extended neurites than LV/GFP-transduced cells (63.75%±8.03% *vs* 16.3%±3.70%, $P<0.01$). LV/DNROCK-transduced DRG neurons had longer neurite length (325.22±10.8 μm *vs* 202.47±9.3 μm, $P<0.01$) and more primary neurites per cell than those in LV/GFP-transduced cells plated on myelin and laminin (7.8±1.25 *vs* 4.84±1.45, $P<0.01$) or on laminin alone (5.2±1.88). LV/DNROCK-transduced cells had significantly larger growth cones (33.12±1.06 μm^2) than LV/GFP-pretreated cells (23.72±1.22 μm^2).

Conclusion: These results indicate that blocking the RhoA/ROCK signaling pathway by expression of DNROCK is effective in facilitating neurite outgrowth in a microenvironment mimicking injury of central nervous system.

Keywords: lentivirus; rho-associated kinases; PC12 cells; dorsal root ganglion neurons; neurites; nerve regeneration; signal transduction

Acta Pharmacologica Sinica (2010) 31: 531–539; doi: 10.1038/aps.2010.35; published online 12 April 2010

Introduction

Most neurons in the adult mammalian CNS do not spontaneously regenerate after injury; this accounts for the persistence of functional deficits in a variety of neurological disorders, including spinal cord injury. This failure is largely attributed to the presence of axonal outgrowth inhibitors in the CNS environment. Myelin-derived inhibitory molecules (for example, Nogo, OMgp, and MAG) and components of the glial scar (*eg*, chondroitin sulphate proteoglycans) form a hostile environment, which prevents regenerating axons from re-establishing functional connections[1]. Many neurite outgrowth inhibitors bind to distinct receptors but their signals converge in the Rho/Rho kinase (ROCK) pathway[2]. RhoA acts as a molecular switch that controls a signal transduction pathway linking transmembrane receptors to the cytoskeleton. In non-neuronal cells, RhoA regulates various cellular processes including formation of stress fibers and focal adhesions, cell motility, cell aggregation, smooth muscle contraction, cytokinesis, and transcriptional regulation through serum response factor[3, 4]. In neurons, RhoA and ROCK have been implicated in transducing signals from neurite outgrowth inhibitors to the actin cytoskeleton of the growth cone as

* To whom correspondence should be addressed.
E-mail cp_yang_1999@yahoo.com
Received 2010-01-05 Accepted 2010-03-03

well as in regulating growth cone collapse and neurite retraction[5–7]. ROCK has previously been shown to be inactivated during neurite outgrowth. Therefore, targeting the RhoA/ROCK signaling pathway is thought to be an attractive strategy for promoting axonal regeneration[8–11]. Pharmacological inhibition of RhoA with C3 transferase or inhibition of ROCK with Y27632 has been shown to stimulate neurite growth on inhibitory substrates in vitro. Inhibition of RhoA or ROCK has also been found to promote regeneration of optic nerves and corticospinal axons *in vivo*[8, 12–15]. However, the clinical use of these antagonists may be limited by undesired side effects and pharmacokinetics. For more sustained inhibition of the Rho/ROCK pathway *in vivo*, the use of dominant negative mutant ROCK to genetically manipulate the molecules involved in the inhibitory cascade might be an effective strategy.

Several dominant negative mutants of ROCK have been identified by Prof Kaibuchi's group[16]. One of these mutants, RB/PH(TT), is composed of the Rho binding (RB) and pleckstrin-homology (PH) domains. This mutant contains two point mutations in the RB domain (Asn-1036 and Lys-1037 to Thr) that abolish its Rho-binding activity. RB/PH(TT) interacts with the catalytic domain of ROCK and specifically inhibits its activity without titrating out RhoA *in vitro*[17, 18], serving as a powerful dominant negative inhibitor[16]. In this study, we placed the cDNA encoding the RB/PH(TT) mutant (referred as DNROCK thereafter) into primary culture neurons or PC12 cell lines by using the lentiviral vector (LV) to study its effects in promoting neurite outgrowth and on growth cone morphology in a mimicking injured CNS environment.

Material and methods

Production of LVs

The myc-RB/Ph(TT) construct of cow Rho kinase α (also called ROCK-II or p160ROCK) was a generous gift from Prof Kaibuchi[16]. The myc-RB/PH(TT) cDNA was excised from the original plasmid and was subcloned into the pRRL lentiviral transfer vector with an IRES-GFP sequence to generate pRRL/myc-RB/PH(TT)-IRES-GFP (pRRL/DNROCK). LVs were produced based on the protocol of Dull *et al* (1998)[19]. Briefly, 10 μg of transfer vector, 6.5 μg of packing vector, and 3.5 μg of envelope vector (VSV-G) were transfected into HEK 293T cells in 10-cm dishes using the calcium precipitation method. After 14 to 16 h, the medium was replaced with 9 mL of media containing 2% fetal bovine serum; conditioned medium was collected 24 h later. Viral vectors were concentrated by centrifugation at 74 000×*g* for 2.5 h at 4 °C in a Sorvall Surespin 630 rotor. The pellet was resuspended in 50 μL PBS. The titer of viral vectors was determined by infection of HEK 293T cells with viral stock diluted by 10^3–10^6 times. Transduced cells expressing GFP were counted to calculate the transduction unit (TU) 48 h after transduction. The titer for LV/DNROCK was in the range of 1×10^8–1×10^9TU/mL. LV carrying the GFP gene (LV/GFP) was produced following the same procedure; the titer of LV/GFP was in the range of 1×10^{10}–1×10^{11} TU/mL.

Assessment of the effects of DNROCK on the cytoskeleton

RhoA/ROCK acts as a molecular switch that receives extracellular signals and controls cytoskeletal behavior. RhoA/ROCK is important for regulating focal adhesion and the formation of stress fibers. We tested whether DNROCK in our system could inhibit ROCK by investigating the intracellular f-actin morphology.

First, to test whether the myc-DNROCK construct with IRES-GFP was able to inhibit ROCK function, a stress fiber formation assay was performed in NIH 3T3 fibroblast cells following serum challenge after serum starvation[20]. NIH 3T3 cells were transfected with either pRRL/DNROCK or pRRL/GFP using Lipofectamine 2000 (Invitrogen, Paisley, UK). After 24 h post-transfection, the cells were starved from serum for 48 h and were then exposed to medium containing 10% fetal bovine serum for 1 h. To detect f-actin, cells were fixed and stained with rhodamine-conjugated phalloidin (Molecular Probes, Invitrogen) according to the manufacturer's instructions.

To test whether LV/DNROCK was also able to inhibit ROCK function, we transduced LV/DNROCK into HeLa cells and examined cell body size as well as phosphorylation of MYPT1 (pMYPT1), a downstream target of ROCK, following serum starvation and serum challenge. As NIH 3T3 cells could not be transduced by LV/DNROCK, we used HeLa cells to test the effects of LV/DNROCK. HeLa cells were transduced with either LV/DNROCK or LV/GFP. After 24 h post-transduction, the cells were starved from serum for 48 h and were then exposed to medium containing 10% fetal bovine serum for 1 h. Next, cells were fixed for f-actin staining or harvested for pMYPT1 immunoblotting. The average area of HeLa was determined using Image J analysis software.

Preparation of crude CNS myelin proteins

To challenge outgrowing axons with a more complex inhibitory environment, dissociated CNS myelin proteins were used as growth substrates for adult rat dorsal root ganglion (DRG) neurons or differentiated PC12 cells. Myelin was purified by two rounds of discontinuous density gradient centrifugation and osmotic disintegration[21]. Solubilized myelin protein was aliquoted and kept at -80 °C. To prepare the myelin substrate, 3 μg/coverslip myelin solution was mixed with 10 μg/mL laminin and was dried overnight onto 13-mm sterile glass coverslips pre-coated with 10 μg/mL poly-*L*-lysine[22].

ROCK activity assay

To verify whether the prepared myelin proteins were able to activate ROCK, which translocates to membrane after activation, and LV/DNROCK could inhibit ROCK activation, differentiated PC12 cells were infected with LV/DNROCK or LV/GFP overnight before being plated on myelin-coated 60-mm culture dishes. One hour later, the cells were collected in cold PBS by gentle scraping and were washed three time; three-quarters of the harvested cells were resuspended in lysis buffer A [50 mmol/L HEPES, 50 mmol/L NaCl, 1 mmol/L

$MgCl_2$, 2 mm EDTA, 0.25 mol/L sucrose with complete protease inhibitors (Roche)]. Cells were sonicated on ice for 15 s, after which they were centrifuged for 10 min at 800×*g* to remove any unlysed cells. The supernatant was then centrifuged at 100 000×*g* for 30 min. Supernatant containing the cytosolic fraction was removed and the membrane fraction-containing pellet was resuspended in lysis buffer B (lysis buffer A with 5% Triton X-100). After 1 h on ice, with stirring every 15 min, the resuspended pellet was centrifuged at 100 000×*g* for 30 min. The supernatant was removed as the membrane fraction. One-fourth of the harvested cells were prepared for measurement of total protein using standard immunoblotting techniques (discussed later). Protein concentration was determined with the Bradford method. ROCK protein content was analyzed by immunoblotting with an anti-ROCK antibody. ROCK levels in the membrane fraction of PC12 cells were analyzed by densitometry using Image J analysis software. Values were normalized to β-actin levels and were expressed as a percentage of ROCK levels in non-stimulated PC12 lysates (control) for each experiment.

Tissue culture and neurite outgrowth assay

All cell culture surfaces were pre-coated with poly-*L*-lysine (0.01%; Sigma-Aldrich) before other coatings were applied and were kept at 4 °C before use. Rat CNS myelin at a concentration of 3.0 μg total protein/coverslip was dried overnight onto 13-mm coverslips and was used as a substrate[22]. Both dissociated adult rat DRG neurons and differentiated PC12 cells were used for neurite outgrowth assays.

Differentiated PC12 cells were plated at 1×10^5–2×10^5/L on poly-*L*-lysine coated 35-mm culture dishes in DMEM with 10% horse serum, 5% fetal bovine serum, and 2 mmol/L *L*-glutamine. PC12 cells were induced with 50 ng/mL nerve growth factor (NGF, 2.5S, Sigma) and were transduced with LV/DNROCK or LV/GFP at final concentration of 10^6 TU/mL. After being cultured overnight at 37 °C with 95% oxygen and 5% CO_2 to allow the expression of the transgene, 2000 cells were plated on each 13-mm coverslip. Coverslips were pre-coated with a mixture of myelin proteins (3 μg/coverslip) or with poly-*L*-lysine alone as control. Forty hours later, the cells were fixed and immunostained with a monoclonal anti-βIII-tubulin antibody (1:1000, Sigma). Images were obtained using a Leica microscope. The length of the longest neurite of each cell and the percentage of neurite-bearing cells were determined from both GFP and βIII-tubulin positive neurons using the Scion image analysis program (Scion Corporation, Frederick, Maryland, USA). In this way, only transduced cells were assessed. Neurons with neurites longer than the diameter of the cell body were recorded as neurite-bearing neurons for the purpose of calculating the percentage of neurite-bearing neurons. About 200 viral vector-transduced cells from each group were measured, and experiments were repeated three times.

To prepare dissociated DRG neurons, DRGs from adult Wistar rats (rats weighed approximately 250 g) were digested with 0.125% collagenase (Type IV, Sigma) in F12 medium for 45 min at 37 °C. Following this incubation, DRGs were digested with 0.25% collagenase for another 45 min. DRGs were washed with F12 medium and were then digested with 0.25% trypsin (Sigma) in F12 medium for 15 min. Trypsinization was stopped by replacing the medium with F12 medium containing 20% fetal calf serum followed by F12 medium alone. DRGs were triturated in 1 mL BSF_2 medium (F-12/DMEM, 1% N-2 supplement (Invitrogen), 0.3% BSA (Fatty acid free, Sigma A-8806), and 100 U/mL penicillin/100 μg/mL streptomycin (Sigma, UK)) and were centrifuged through a cushion of 2 mL 15% BSA (Sigma, A-9576 or A-8327) at 900 r/min for 10 min. The cell pellet was resuspended in BSF_2 and was transduced with LV/DNROCK or LV/GFP at a final concentration of 10^6 TU/mL. Neurons were cultured overnight (37 °C with 95% O_2 and 5% CO_2) on a 35-mm culture dish pre-coated with PLL and Laminin. Neurons were then dissociated and plated at 1500 cells/coverslip onto coverslips pre-coated with a mixture of myelin proteins (3 μg/coverslip) and laminin (10 μg/mL, Sigma, UK) or laminin alone as control. Forty hours later, the neurons were fixed in 4% (*w/v*) paraformaldehyde and were immunostained with a polyclonal GAP-43 antibody (for LV/GFP transduced neurons) and a monoclonal c-myc antibody (for LV/DNROCK transduced neurons). Using the Scion image analysis program, we determined the length of the longest neurite, the percentage of neurite-bearing neurons, or the total process outgrowth for LV/GFP transduced neurons positive for both GAP-43 and GFP. We also measured these parameters for LV/DNROCK transduced neurons positive for both GAP-43 and myc. About 200 viral vector-transduced cells from each group were measured. Experiments were repeated three times.

Effect of DNROCK on growth cone morphology

For growth cone collapse experiments, differentiated PC12 cells transduced with LV/DNROCK or LV/GFP were treated with 50 ng/mL NGF overnight before being plated on myelin substrates (3 μg/coverslip). After 16 h in culture, the cells were fixed and stained with rhodamine-conjugated phalloidin (Molecular Probes, Invitrogen) according to the manufacturer's instructions. Fluorescent images of growth cones were captured with a 100×oil immersion objective. Quantification of growth cone area was derived from at least 30 isolated growth cones per treatment with Image J software. A growth cone was defined as the enlarged area distal to where the initial splaying of the axon began, including all lamellipodia and filopodia.

Immunocytochemistry

Cells were fixed with 4% (*w/v*) paraformaldehyde and were blocked with 10% normal donkey serum (Jackson Immunoresearch) in 0.1 mol/L PBS for 20 min. Cells were then incubated with primary antibodies overnight at 4 °C. Fluorescence conjugated secondary antibodies were applied for 2 h at room temperature. After washing, coverslips were mounted on slides with glycerol and PBS (9:1) containing 2.5% DABCO (Sigma). The primary antibody was omitted in the control group. The following primary antibodies were used: anti-c-

myc monoclonal antibody (1:1000, Cell Signaling, New England Biolabs), anti-βIII-tubulin monoclonal antibody (1:1000, Sigma), and anti-GAP-43 polyclonal antibody (1:10 000, gift from Prof JV Priesterly). The secondary antibodies used were FITC conjugated donkey anti-rabbit or anti-mouse IgG (1:400, Jackson Immunoresearch) and TRITC conjugated donkey anti-rabbit or anti-mouse IgG (1:400, Jackson Immunoresearch).

Immunoblotting assay

Cells grown in 35-mm tissue culture dishes were collected in cold PBS with gentle scraping and were washed three times. Cells were then resuspended in lysis buffer containing 20 mmol/L Tris-HCl, 150 mmol/L NaCl, 2 mmol/L EDTA, 0.1 mmol/L EGTA, 1% Triton X-100, and 0.5% deoxyocholine with complete protease inhibitors (Roche). Samples were kept on ice for 30 min and were then centrifuged at 13 000×*g* for 15 min to remove cell debris. Protein concentration in supernatants was determined with the Bradford assay using bovine serum albumin as a standard. Twenty micrograms of protein was subjected to 10% sodium dodecyl sulfate polyacrylamide gel electrophoresis using dual color protein standards (Bio-Rad) as markers. After protein transfer, the polyvinylidene difluoride membrane was blocked with 5% nonfat milk in Tris-buffered saline with 0.1% Tween-20 for 1 h. Membranes were probed with primary antibodies overnight at 4 °C and a peroxidase-conjugated secondary antibody (1:10 000 diluted, ECL Blotting Pack, Amersham, GE Healthcare) was applied for 2 h at room temperature. Immunosignals were detected using the ECL Plus kit (GE Healthcare, Chalfont St Giles, United Kingdom). Primary antibodies used included anti-c-myc monoclonal antibody (1:1000, Cell Signaling, New England Biolab), anti-GFP polyclonal antibody (1:500, Chemicon), and anti pMYPT1 polyclonal antibody (1:1000, Upstate). Anti-β-actin monoclonal antibody was used as an internal control for quantification of bands. Bands were analyzed by densitometry using Image J analysis software.

Statistical methods

The data are expressed as the mean±standard error of the mean (SEM). Statistical analysis consisted of applying a *t* test and using ANOVA to compare two or more groups. Differences were considered to be significant when $P<0.05$.

Results

Effect of DNROCK on the cytoskeleton

Formation of stress fibers in NIH 3T3 cells following serum starvation and serum challenge is a process mediated by the RhoA/ROCK signaling pathway. In untransfected cells or in cells transfected with pRRL/GFP, serum-induced formation of stress fibers was clearly visible (Figure 1A–1C). No obvious differences in morphology or in stress fiber densities could be discerned between pRRL/GFP-transfected and untransfected cells (data not shown). However, cells expressing DNROCK displayed flattened morphology and elongated processes with very few visible stress fibers (Figure 1D–1F). These data indicate that the DNROCK construct with IRES-GFP effectively inhibits the RhoA/ROCK signaling pathway, as demonstrated with a myc-tagged DNROCK construct previously reported[16]. Quantification of stress fibers by densitometry is shown in Figure 1G. Statistical analysis using one-way analysis of variance (ANOVA) for optic density demonstrates a significant difference between the two groups ($P<0.01$).

LV/DNROCK-transduced HeLa cells showed larger cell body size (Figure 2D–2F) than LV/GFP-transfected cells (Figure 2A–2C). LV/DNROCK-transduced HeLa cell bodies were almost twice as large (4124.46±955.68 μm^2) as LV/GFP-transduced cell bodies (2063.21±892.34 μm^2; $P<0.01$; Figure 2G). Following serum starvation and serum challenge, DNROCK also decreased phosphorylation levels of MYPT1, which is normally phosphorylated by ROCK (Figure 2H).

LV-mediated transgene expression in PC12 cells and cultured DRG neurons

PC12 cells expressed GFP after being transduced with either LV/GFP or LV/DNROCK. Bright GFP fluorescence was observed in almost all cells, even those cultured for only 16 h (Figure 3A). In LV/DNROCK-transduced PC12 cells, GFP fluorescence could also be directly visualized, but fluorescence was slightly weaker as compared to LV/GFP-transduced cells (72 h culture; Figure 3B). Immunostaining and immunoblotting showed that PC12 cells transduced with LV/DNROCK expressed high levels of myc-RB-PH(TT) (Figure 3C–3D), while cells transduced with LV/GFP did not express myc-RB-PH(TT) protein (Figure 3D). On immunoblots (Figure 3D), a 55 kDa band was identified that matched the predicted molecular weight of the myc-tagged DNROCK protein.

In primary cultures of DRG neurons, GFP expression in LV/DNROCK-transduced neurons was too weak to be visualized directly 48 h after transduction. GFP expression could be verified by anti-GFP antibody immunoblotting (Figure 3F), while DNROCK expression could be identified by immunostaining with an anti-myc antibody (Figure 3E). DNROCK molecules were present in all parts of the neurons from the somata to the growth cones. DNROCK expression was also detected in immunoblots. These experiments showed that LV/DNROCK-transduced DRG neurons expressed myc-RB-PH(TT) and lower levels of GFP, while LV/GFP-transduced neurons expressed relatively high levels of GFP (Figure 3F).

DNROCK inhibits the translocation of ROCK from cytosol to membrane

The inactive form of ROCK predominates in the cytoplasm and is translocated to the membrane upon Rho-mediated activation. Binding of ROCK to the membrane may represent ROCK activation. To test if myelin protein could activate ROCK and to test whether DNROCK was able to block ROCK activation, differentiated PC12 cells were infected with LV/DNROCK or LV/GFP overnight before being plated on a myelin substrate. We found that myelin protein significantly increased translocation of ROCK from cytosol to membrane in LV/GFP-treated PC12 cells, whereas LV/DNROCK blocked ROCK translocation (Figure 4A–4B).

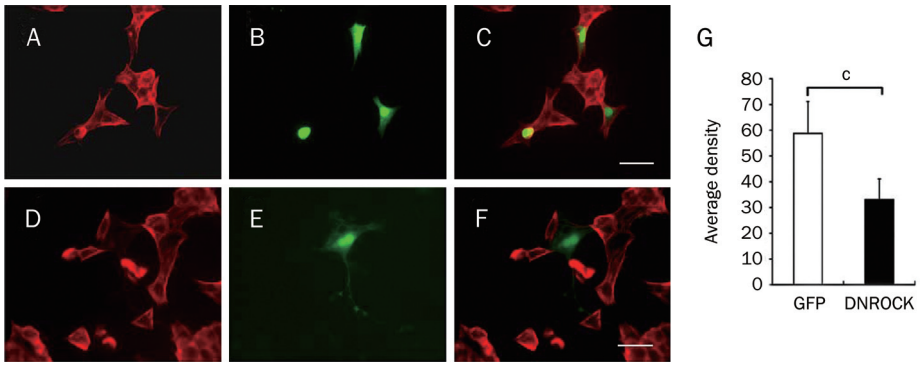

Figure 1. Effect of pRRL/DNROCK on actin stress fiber formation in NIH 3T3 cells. NIH 3T3 cells were transfected with either pRRL/GFP (A–C) or pRRL/DNROCK (D–F). After 24 h post-transfection, cells were starved from serum for 48 h and were then transferred to medium containing 10% fetal bovine serum for 1 h. F-actin was stained with rhodamine-conjugated phalloidin (red in A, C, D, F). Cells transfected with LV/DNROCK looked flattened with extended processes and lacked stress fibers (D and F). In cells transfected with pRRL/GFP, stress fibers were clearly visible (A and C). (G) Quantification of stress fibers by densitometry. Data presented are mean±SEM. Density was measured in arbitrary units with Image J, and the corresponding background signals were subtracted. $^{c}P<0.01$. Scale bar=50 μm; DNROCK, dominant negative Rho kinase; GFP, green fluorescent protein.

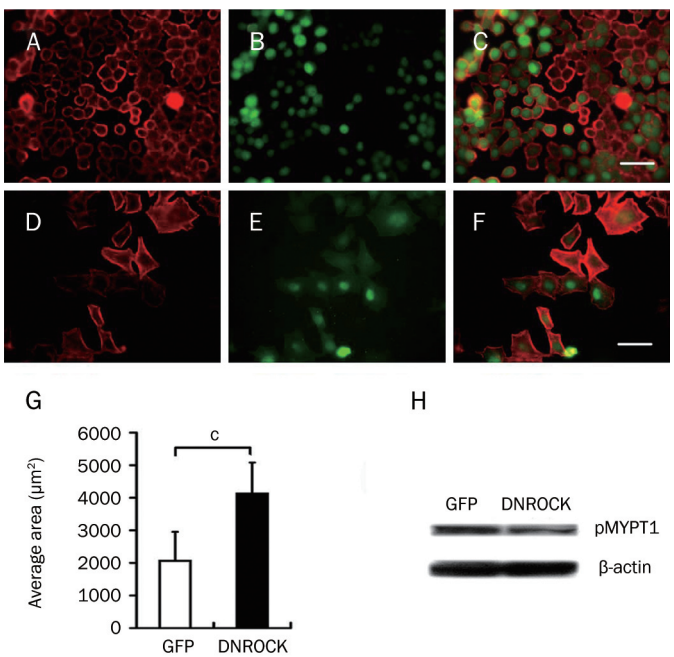

Figure 2. Effect of LV/DNROCK on morphology of Hela cells and ROCK downstream targets. Hela cells were transduced with either LV/GFP (A–C) or pRRL/DNROCK (D–F). After 24 h, cells were starved from serum for 48 h and were then transduced in medium containing 10% fetal bovine serum for 1 h. F-actin was stained with rhodamine-conjugated phalloidin (red in A, C, D, F). LV/DNROCK-transduced cells showed larger cell body size (D–F) than LV/GFP-transduced cells (A–C). (G) Quantification of average area. Values are represented as mean±SEM. $^{c}P<0.01$. Scale bar=50 μm. (H) Immunoblotting shows that DNROCK decreased MYPT1 phosphorylation levels following serum challenge after serum starvation.

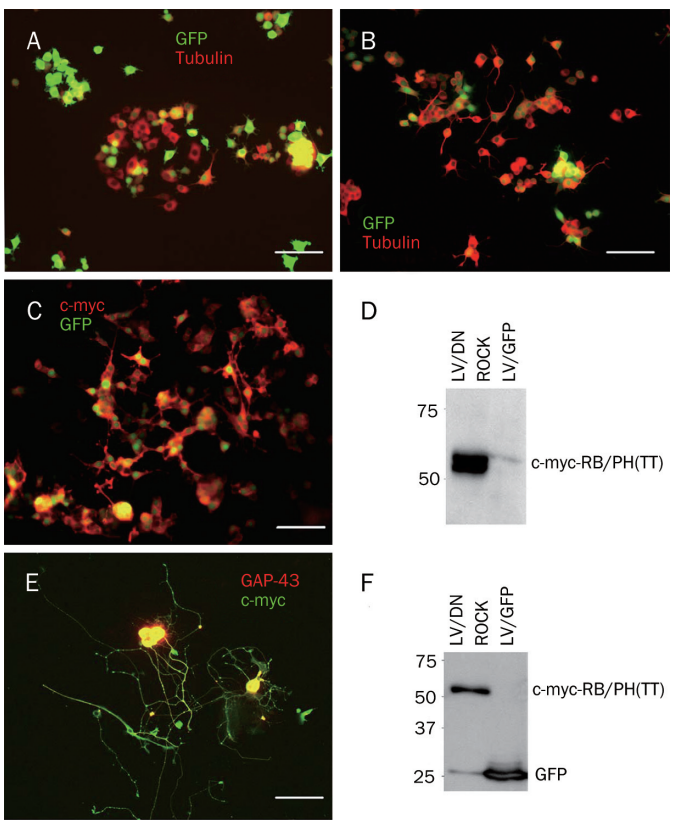

Figure 3. Lentivirus-mediated expression of DNROCK in PC12 cells and DRG neurons. (A) Expression of GFP in PC12 cells transduced with LV/GFP for 16 h. (B) Expression of GFP in PC12 cells transduced with LV/DNROCK for 72 h. (C) Expression of DNROCK in LV/DNROCK-transduced PC12 cells detected using anti-myc antibody. (D) Expression of c-myc in LV/DNROCK-transduced PC 12 cells detected by immunoblotting. (E) Expression of DNROCK in LV/DNROCK-transduced DRG neurons detected using anti-c-myc antibody. (F) Immunoblotting using anti-c-myc and anti-GFP antibodies detected expression of DNROCK and GFP proteins in viral vector-transduced DRG neurons. Scale bar=100 μm

DNROCK promotes neurite outgrowth of differentiated PC12 cells on myelin protein

After being seeded on PLL-coated coverslips for 48 h, 54.5%

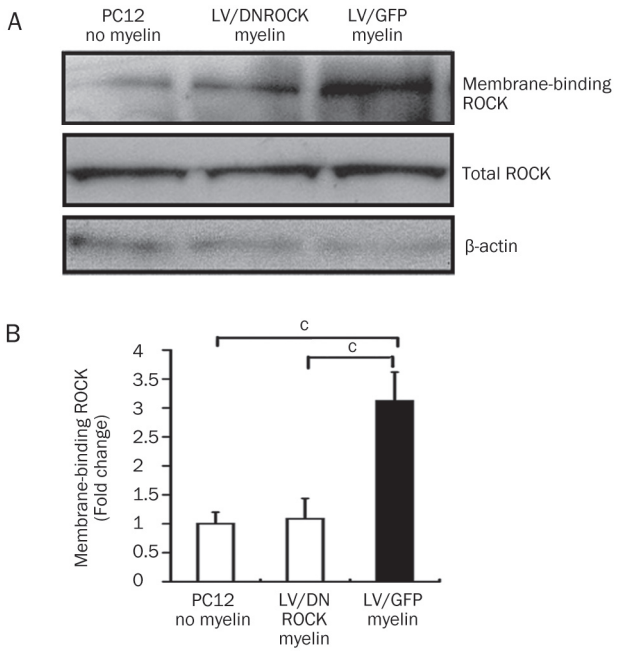

Figure 4. LV/DNROCK blocked the translocation of ROCK. (A) Myelin protein induces ROCK translocation to the membrane. Myelin treatment increased translocation of ROCK from cytosol to membrane in the LV/GFP-treated group, whereas LV/DNROCK blocked the translocation of ROCK. (B) Quantification of membrane-bound ROCK by densitometry using Image J. Values are represented as mean±SEM. $^{c}P<0.01$.

of LV/GFP-transduced PC12 cells grew neurites with an average length of 45.4±2.5 μm (Figure 5A, 5D–5E), comparable to values for non-LV-transduced PC12 cells (data not shown). Non-transduced or LV/GFP-transduced PC12 cells seeded on myelin-coated coverslips showed reduced neurite outgrowth; many cell bodies remained round-shaped and lacked neurites (Figure 5B). About 16% of LV/GFP-transduced cells grew neurites, which is significantly less than neurite growth observed in cells plated on PLL-coated coverslips (Figure 5E). Neurite length was also significantly shorter in cells plated on myelin (29.3±1.7 μm) than in cells plated on PLL-coated coverslips (45.4±2.5 μm; Figure 5D). It should be noted that only neurites longer than the diameter of the cell body were measured. As a result, the observed reduction of neurite length by myelin protein appears less dramatic. These results confirm that dissociated myelin protein can profoundly inhibit neurite outgrowth of differentiated PC12 cells. However, LV/DNROCK-transduced PC12 cells growing on myelin-coated coverslips had longer neurites than LV/GFP-transduced cells (LV/DNROCK: 39.18±2.19 μm; LV/GFP: 29.32±1.7 μm; Figure 5B–5D). Furthermore, a significantly higher percentage of LV/DNROCK-transduced cells extended neurites than LV/GFP-transduced cells (LV/DNROCK: 63.75%±8.03%; LV/GFP: 16.3%±3.70%). When compared with cells growing on PLL-coated coverslips, neurite length was shorter in LV/DNROCK-transfected cells. However, the percentage of cells bearing neurites was comparable to that of the control group (LV/DNROCK: 63.75%±8.03%; LV/GFP: 54.5%±6.39%; Figure 5D–5E).

DNROCK promotes neurite outgrowth in DRG neurons cultured on myelin protein

After being plated for 40 h on laminin-coated coverslips, LV/GFP-transduced DRG neurons grew long neurites (433.86±18.78 μm). In addition, 95% of LV/GFP-transduced DRG neurons plated on laminin grew neurites (Figure 6A, 6D–6E), resembling non-LV-transduced DRG neurons (data not shown). Myelin protein significantly reduced neurite length in LV/GFP-transduced cells (202.47±9.3 μm) and also reduced the percentage of neurite-bearing cells to 36% (Figure 6B, 6D–6E). Expression of DNROCK in DRG neurons overcame the effects of myelin protein. Neurite length of LV/DNROCK-transduced cells was much longer (325.22±10.8 μm) as compared with LV/GFP-transduced cells plated on myelin, although neurites were still shorter than those of cells growing on laminin (Figure 6C–6D). The percentage of neurite-bearing cells was also significantly increased in these cells as compared to LV/GFP-transduced cells (Figure 6E). Interestingly, LV/DNROCK-transduced cells had more primary neurites (7.8±1.25) per cell than LV/GFP-transduced cells plated on myelin and laminin (4.84±1.45) or on laminin alone (5.2±1.88; Figure 6F; see higher magnification image in this figure). However, myelin protein did not affect the number of primary neurites per neuron (Figure 6F).

DNROCK alters growth cone morphology

Growth cones were characterized by the presence of many long filopodia and by a relative lack of actin bundles in the central domain (Figure 7A–7D). LV/DNROCK-transduced cells had significantly larger growth cones (33.12±1.06 μm^2) than LV/GFP-pretreated cells (23.72±1.22 μm^2). Growth cones of LV/GFP-transduced cells were similar to those of non-transduced cells (data not shown).

Discussion

Most neurite outgrowth inhibitors exert inhibitory effects by signaling through the RhoA/ROCK pathway, eventually converging to the actin cytoskeleton (for review see Suter and Forscher, 2000)[23]. RhoA/ROCK is activated by MAG, Nogo-66, and oligodendrocyte-myelin glycoprotein through a $p75^{NTR}$-dependent mechanism. In its active, GTP-bound form, RhoA/ROCK rigidifies the actin cytoskeleton, thereby inhibiting axon elongation and mediating growth cone collapse. In this way, RhoA/ROCK signaling inhibits neurite outgrowth. Consequently, targeting the RhoA/ROCK signaling pathway is thought to be an effective way to promote axon regeneration following CNS injury. Many *in vitro* and *in vivo* studies using RhoA inhibitors (C3 or its cell-permeable derivatives C3-05, C3-07, BA-210) or ROCK inhibitors (Y27632 or Fasudil) have demonstrated the effectiveness of targeting this signal pathway[24]. In this study, we report that DNROCK could block this pathway and promote neurite outgrowth in an inhibitory CNS microenvironment. We manipulated the RhoA/ROCK

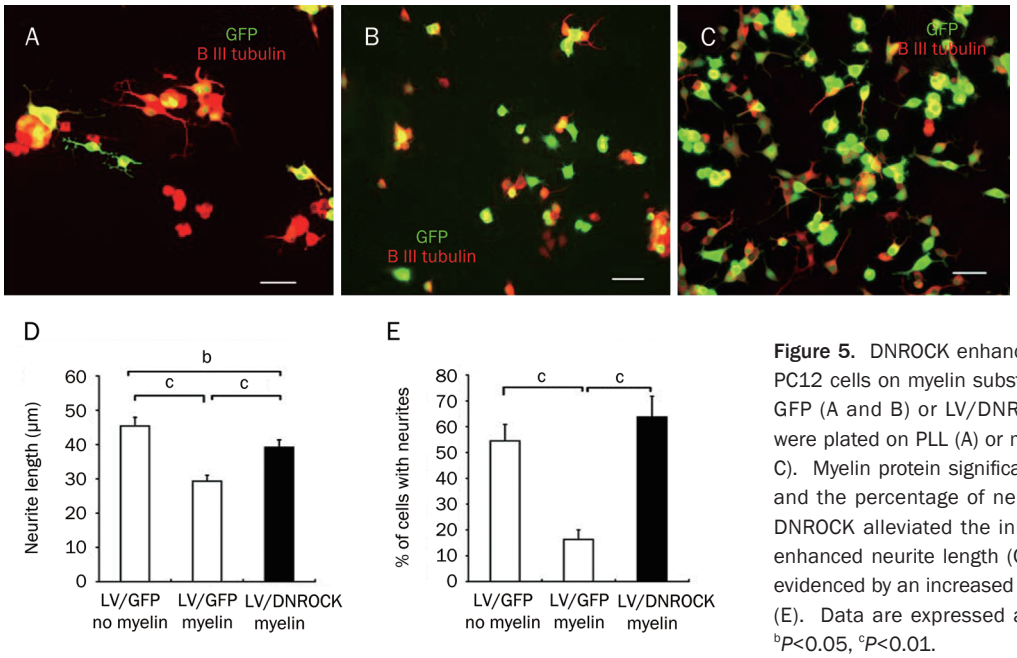

Figure 5. DNROCK enhances neurite outgrowth of differentiated PC12 cells on myelin substrate. PC12 cells transduced with LV/GFP (A and B) or LV/DNROCK (C) were treated with NGF and were plated on PLL (A) or myelin protein-coated coverslips (B and C). Myelin protein significantly reduced neurite length (B and D) and the percentage of neurite-bearing cells (E). Expression of DNROCK alleviated the inhibitory effects of myelin protein and enhanced neurite length (C and D) and sprouting of neuritis, as evidenced by an increased percentage of neurite-bearing neurons (E). Data are expressed as mean±SEM. Scale bars=100 μm. $^{b}P<0.05$, $^{c}P<0.01$.

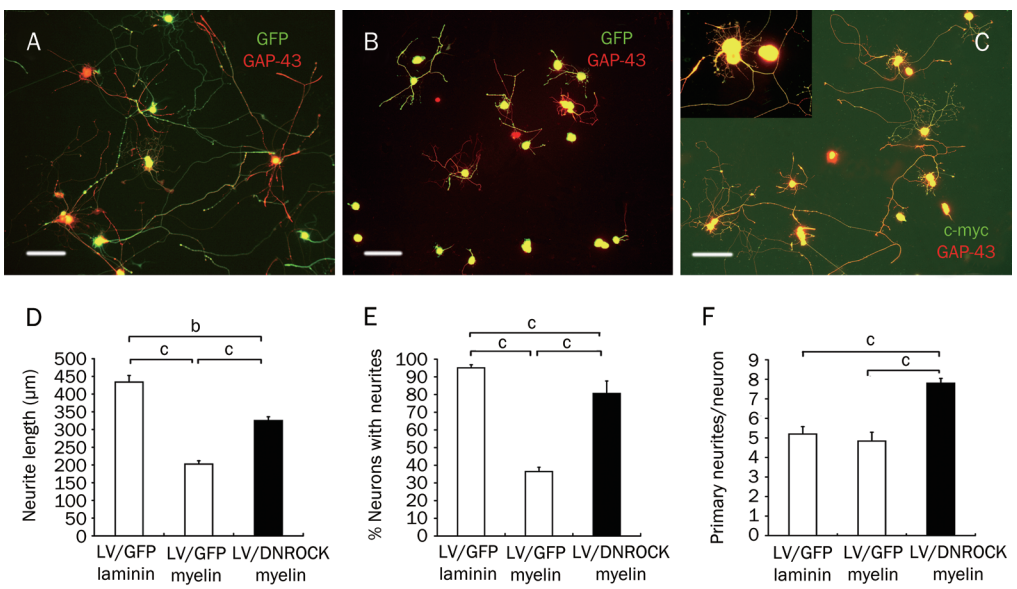

Figure 6. DNROCK enhances neurite outgrowth of DRG neurons on myelin substrate. Dissociated DRG neurons transduced with LV/GFP (A and B) or LV/DNROCK (C) were plated on laminin (A) or laminin+myelin protein (B and C)-coated coverslips. Myelin protein significantly reduced neurite length (B and D) and the percentage of neurite-bearing neurons (E) but did not affect the number of neurites per neuron (F) in LV/GFP-transduced neurons. Expression of DNROCK reversed the effects of myelin and enhanced neurite length (C and D) and sprouting of neurites (E), with increased number of neuritis per neuron (F). Values are expressed as mean±SEM. Scale bars=100 μm. $^{b}P<0.05$, $^{c}P<0.01$.

signaling pathway by LV delivery of DNROCK to neurons. DNROCK expression in PC12 cells and in primary DRG neurons increased the chances that cells would initiate neurites. DNROCK also increased mean neurite length and growth cone size on multiple myelin-associated inhibitory substrates. The evidence presented in this paper demonstrates that ROCK inactivation promotes the outgrowth of neurites over myelin substrates in vitro, consistent with previously published results[2, 8, 12].

The DNROCK construct RB/PH(TT) has been shown to be one of the most potent dominant negative mutants in blocking the RhoA/ROCK pathway[16]. Expression of this mutant inhibits lysophosphatidic acid-induced neurite retraction in N1E-115 neuroblastoma cells and inhibits serum-induced myosin light chain phosphorylation in NIH 3T3 cells[16]. In the current study, we showed that expression of DNROCK in

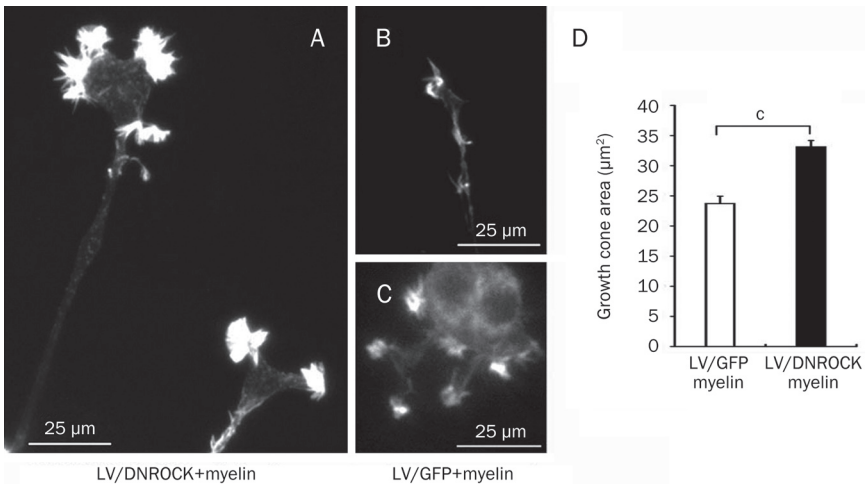

Figure 7. DNROCK alters growth cone morphology. LV/DNROCK-transduced cells had significantly larger growth cones (A) than LV/GFP-transduced cells (B and C). Quantification of growth cone size (D). Values are expressed as mean±SEM. Scale bars=25 μm. $^{c}P<0.01$.

NIH 3T3 cells significantly reduces serum-induced formation of stress fibers, which is in agreement with results obtained by direct injection of maltose-binding protein-fused RB/PH(TT) into Madin-Darby canine kidney epithelial cells[17, 25]. When expressed in PC12 cells and in adult rat dissociated DRG neurons, DNROCK significantly inhibits the effects of myelin protein and promotes neurite initiation and elongation.

Crude CNS myelin substrates prepared from rat brain contain several inhibitors that block neurite outgrowth[26, 27]. We have demonstrated that ROCK inhibition stimulates axonal outgrowth over myelin substrates. The difference in the percentage of neurite-bearing cells between GFP and DNROCK groups was far more striking than the difference in neurite length between GFP and DNROCK groups. We also observed that DNROCK-expressing DRG neurons extended more neurites per cell than both in the control group and in the GFP group (Figure 6F), indicating that the Rho/ROCK signaling pathway normally regulates neuritogenesis by suppression of branching initiation. Such a phenomenon was also observed by Bito, who found exuberant axonal processes in cultured cerebellar granule neurons after inhibition of the RhoA/ROCK pathway using C3 or Y27632[28]. Taken together, these results indicate that the RhoA/ROCK signaling pathway may be an important factor in growth cone signaling induced by myelin-associated inhibitors. The RhoA/ROCK pathway may also function as a gate controlling the initiation of neuritogenesis.

ROCK was shown to negatively control the size and motility of axonal growth cones. Axonal growth inhibition is accompanied by distinct changes in growth cone behavior and morphology, mediated primarily through the action of the Rho family of small GTPases that signal modulation of polymerization of the actin cytoskeleton[29]. Growth cones are highly motile structures that interpret extracellular signals and lead neurites to appropriate targets. Positive guidance cues promote the accumulation of f-actin in the peripheral area of the growth cone at the site of contact[30]. In central regions of the growth cone, actin is depleted. This is thought to be necessary to allow the invasion of microtubules, enabling consolidation of the axon[31] and leading to a larger growth cone. Inhibition cues, on the other hand, induce the redistribution of actin from the periphery to the center of the growth cone. This may hamper the invasion of microtubules and may cause growth cone collapse by activating RhoA/ROCK[32]. Thus, RhoA/ROCK-mediated negative regulation of actin dynamics at the soma and in growth cones may be critical to regulation of axon numbers and growth cone size[28]. In the current study, we showed that DNROCK expression in PC12 cells and in primary DRG neurons led to larger growth cones and higher numbers of primary neurites per cell than in control as well as LV/GFP-transduced neurons. These results are in agreement with those obtained by Bito[28].

In conclusion, the results of the present study suggest that lentiviral-mediated DNROCK transfection in adult dissociated DRG neurons and in PC12 cells can promote neurite outgrowth as well as neuritogenesis in an inhibitory environment that mimics the injured CNS. These results are consistent with those reported in our previously published study[33]. In the current study, we tested whether a different promoter of DNROCK could affect its effects on neurite outgrowth, stress fiber formation, and growth cone morphology. These results demonstrated that the c-myc promoter could also promote DNROCK expression, which subsequently overcame a microenvironment mimicking the injured CNS and promoted neurite outgrowth. DNROCK expression also increased the size of HeLa cells and growth cones by affecting actin cytoskeleton dynamics. These results additionally showed that DNROCK could not completely block the inhibition of neurite growth by myelin protein. Thus, it cannot be ruled out that other Rho and ROCK effectors (*eg*, p140mDia, protein kinase N, and myosin light chain kinase) might also be involved in CNS neurite inhibition. We should note that the failure of adult mammalian CNS regeneration can also partially be attributed to the following: (1) an absence of permissive substrates to support axonal attachment and extension through lesion sites, (2) a lack of neurotrophic stimulation, (3) myelin-based and extracellular matrix inhibitors in the injured region, (4) partial deficiency in the intrinsic growth capacity of adult neurons, and (5) extensive secondary damage result-

ing from inflammatory mechanisms[34]. In order to get more successful regeneration, a combination of strategies should be used. We therefore suggest that disinhibition alone may not be sufficient to promote optimum CNS axon growth. Injured neurons may also require activation through, for example, either NTF or cAMP stimulation, to effect maximal possible survival and regeneration, as previously suggested[35, 36].

Acknowledgements

We thank Dr Xuenong BO for the LV plasmids and for technical assistance. This work was supported by a grant from the National Ministry of Education and the Third Military Medical University of China.

Author contribution

Ping YANG designed and performed the research, analyzed data and wrote the paper. Hui-zhong WEN helped for the data analysis and experiment preparation. Jin-hai ZHANG helped for the experimental manage.

References

1 Fawcett JW. Overcoming inhibition in the damaged spinal cord. J Neurotrauma 2006; 23: 371–83.
2 Alabed YZ, Grados-Munro E, Ferraro GB, Hsieh SH, Fournier AE. Neuronal responses to myelin are mediated by Rho kinase. J Neurochem 2006; 96: 1616–25.
3 Etienne-Manneville S, Hall A. Rho GTPases in cell biology. Nature 2002; 420: 629–35.
4 Kaibuchi K. Phosphorylation of myosin-binding subunit (MBS) of myosin phosphatase by Rho-kinase *in vivo*. J Cell Biol 1999; 147: 1023–38.
5 Nikolic M. The role of Rho GTPases and associated kinases in regulating neurite outgrowth. Int J Biochem Cell Biol 2002; 34: 731–45.
6 Filbin MT. Myelin-associated inhibitors of axonal regeneration in the adult mammalian CNS. Nat Rev Neurosci 2003; 4: 703–13.
7 Hu F, Strittmatter SM. Regulating axon growth within the postnatal central nervous system. Semin Perinatol 2004; 28: 371–8.
8 Lehmann M, Fournier A, Selles-Navarro I, Dergham P, Sebok A, Leclerc N, *et al*. Inactivation of Rho signaling pathway promotes CNS axon regeneration. J Neurosci 1999; 19: 7537–47.
9 Schwab ME. Nogo and axon regeneration. Curr Opin Neurobiol 2004; 14: 118–24.
10 Ellezam B, Dubreuil C, Winton M, Loy L, Dergham P, Selles-Navarro I, *et al*. Inactivation of intracellular Rho to stimulate axon growth and regeneration. Prog Brain Res 2002; 137: 371–80.
11 Schwab JM, Brechtel K, Mueller CA, Failli V, Kaps HP, Tuli SK, *et al*. Experimental strategies to promote spinal cord regeneration — an integrative perspective. Prog Neurobiol 2006; 78: 91–116.
12 Dergham P, Ellezam B, Essagian C, Avedissian H, Lubell WD, McKerracher L. Rho signaling pathway targeted to promote spinal cord repair. J Neurosci 2002; 22: 6570–7.
13 Fournier AE, Takizawa BT, Strittmatter SM. Rho kinase inhibition enhances axonal regeneration in the injured CNS. J Neurosci 2003; 23: 1416–23.
14 Bertrand J, Winton MJ, Rodriguez-Hernandez N, Campenot RB, McKerracher L. Application of Rho antagonist to neuronal cell bodies promotes neurite growth in compartmented cultures and regeneration of retinal ganglion cell axons in the optic nerve of adult rats. J. Neurosci 2005; 25: 1113–21.
15 Lingor P, Teusch N, Schwarz K, Mueller R, Mack H, Bahr M. Inhibition of Rho kinase (ROCK) increases neurite outgrowth on CSPG *in vitro* and axonal regeneration in the adult optic nerve *in vivo*. J Neurochem 2007; 103: 181–9.
16 Amano M, Chihara K, Nakamura N, Fukata Y, Yano T, Shibata M, *et al*. Myosin II activation promotes neurite retraction during the action of Rho and Rho-kinase. Genes Cells 1998; 3: 177–88.
17 Amano M, Chihara K, Nakamura N, Kaneko T, Matsuura Y, Kaibuchi K. The COOH terminus of Rho-kinase negatively regulates Rho-kinase activity. J Biol Chem 1999; 274: 32418–24.
18 Amano M, Fukata Y, Kaibuchi K. Regulation and functions of Rho-associated kinase. Exp Cell Res 2000; 261: 44–51.
19 Dull T, Zufferey R, Kelly M, Mandel RJ, Nguyen M, Trono D, *et al*. A third-generation lentivirus vector with a conditional packaging system. J Virol 1998; 72: 8463–71.
20 Ridley AJ, Hall A. Signal transduction pathways regulating Rho-mediated stress fibre formation: requirement for a tyrosine kinase. J EMBO 1994; 13: 2600–10.
21 Norton WT, Poduslo SE. Myelination in rat brain: method of myelin isolation. J Neurochem 1973; 21: 749–57.
22 Mukhopadhyay G, Doherty P, Walsh FS, Crocker PR, Filbin MT. A novel role for myelin-associated glycoprotein as an inhibitor of axonal regeneration. Neuron 1994; 13: 757 – 67.
23 Suter DM, Forscher P. Substrate-cytoskeletal coupling as a mechanism for the regulation of growth cone motility and guidance. J Neurobiol 2000; 44: 97–113.
24 McKerracher L, Higuchi H. Targeting Rho to stimulate repair after spinal cord injury. J Neurotrauma 2006; 23: 309–17.
25 Kawano Y, Fukata Y, Oshiro N, Amano M, Nakamura T, Ito M, *et al*. Phosphorylation of myosin-binding subunit (MBS) of myosin phosphatase by Rho-kinase *in vivo*. J Cell Biol 1999; 147: 1023–38.
26 Gao Y, Deng K, Hou J, Bryson JB, Barco A, Nikulina E, *et al*. Activated CREB is sufficient to overcome inhibitors in myelin and promote spinal axon regeneration *in vivo*. Neuron 2004; 44: 609–21.
27 Ahmed Z, Dent RG, Suggate EL, Barrett LB, Seabright RJ, Berry M, *et al*. Disinhibition of neurotrophin-induced dorsal root ganglion cell neurite outgrowth on CNS myelin by siRNA-mediated knockdown of NgR, p75NTR and Rho-A. Mol Cell Neurosci 2005; 28: 509–23.
28 Bito H, Furuyashiki T, Ishihara H, Shibasaki Y, Ohashi K, Mizuno K, *et al*. A critical role for a Rho-associated kinase, p160ROCK, in determining axon outgrowth in mammalian CNS neurons. Neuron 2000; 26: 431–41.
29 Luo L. Rho GTPases in neuronal morphogenesis. Nat Rev Neurosci 2000;1: 173–80.
30 Lin CH, Forscher P. Cytoskeletal remodeling during growth cone-target interactions. J Cell Biol 1993; 21: 1369–83.
31 Suter DM, Forscher P. An emerging link between cytoskeletal dynamics and cell adhesion molecules in growth cone guidance. Curr Opin Neurobiol 1998; 8: 106–16.
32 Nobes CD, Hall A. Rho, rac and cdc42 GTPases: regulators of actin structures, cell adhesion and motility. Biochem Soc Trans 1995; 23: 456–9.
33 Wu DS, Yang P, Zhang XY, Luo J, Haque ME, Yeh J, *et al*. Targeting a dominant negative rho kinase to neurons promotes axonal outgrowth and partial functional recovery after rat rubrospinal tract lesion. Mol Ther 2009; 17: 2020–30.
34 Kadoya K, Tsukada S, Lu P, Coppola G, Geschwind D, Filbin MT, *et al*. Combined intrinsic and extrinsic neuronal mechanisms facilitate bridging axonal regeneration one year after spinal cord injury. Neuron 2009; 4: 165–72.
35 Fischer D, Petkova V, Thanos S. Switching mature retinal ganglion cells to a robust growth state *in vivo*: gene expression and synergy with RhoA inactivation. J Neurosci 2004; 24: 8726–40.
36 Pearse DD, Pereira FC, Marcillo AE. cAMP and Schwann cells promoter axonal growth and functional recovery after spinal cord injury. Nature 2004; 10: 610–6.